Marine Geodesy
Publication details, including instructions for authors and subscription information:
http://www.tandfonline.com/loi/umgd20

Automatic Registration of Coastal Remotely Sensed Imagery by Affine Invariant Feature Matching with Shoreline Constraint

Liang Cheng [a b], Lihua Tong [a b], Yongxue Liu [a b], Manchun Li [a b] & Jiechen Wang [a b]

[a] Jiangsu Provincial Key Laboratory of Geographical Information Science and Technology, Nanjing University, Nanjing, China

[b] Collaborative Innovation Center for the South China Sea Studies, Nanjing University, Nanjing, China

Published online: 04 Mar 2014.

To cite this article: Liang Cheng, Lihua Tong, Yongxue Liu, Manchun Li & Jiechen Wang (2014) Automatic Registration of Coastal Remotely Sensed Imagery by Affine Invariant Feature Matching with Shoreline Constraint, Marine Geodesy, 37:1, 32-46, DOI: 10.1080/01490419.2013.868382

To link to this article: http://dx.doi.org/10.1080/01490419.2013.868382

Marine Geodesy, 37:32–46, 2014

ISSN: 0149-0419 print / 1521-060X online
DOI: 10.1080/01490419.2013.868382

Taylor & Francis
Taylor & Francis Group

Automatic Registration of Coastal Remotely Sensed Imagery by Affine Invariant Feature Matching with Shoreline Constraint

LIANG CHENG,[1,2] LIHUA TONG,[1,2] YONGXUE LIU,[1,2] MANCHUN LI,[1,2] AND JIECHEN WANG[1,2]

[1]Jiangsu Provincial Key Laboratory of Geographical Information Science and Technology, Nanjing University, Nanjing, China
[2]Collaborative Innovation Center for the South China Sea Studies, Nanjing University, Nanjing, China

A new approach based on Affine Invariant Feature Matching (AIFM) with a filtering technique is proposed for automatic registration of remotely sensed image in coastal areas. The novelty of this approach is an automatic filtering technique using RANdom SAmple Consensus (RANSAC) with shoreline constraint for AIFM to remove all wrong matches and simultaneously keep as many correct matches as possible. To implement it, a progressive threshold strategy (from small value to large value) is presented to determine an appropriate RANSAC threshold, in which the progressive process is guided by shoreline constraint. The proposed approach (with filtering) is compared with standard AIFM (without filtering) using two typical image pairs in coastal areas. The experimental results indicate that the proposed approach can always provide much better matching results than standard AIFM.

Keywords Coastal remote sensing, image registration, affine invariant matching, filtering, shoreline constraint

Introduction

Coastal mapping and change monitoring become critical to safe navigation, coastal resource management, coastal environmental protection, and sustainable coastal development (Li et al. 2002, 2008). Availability of multisensor and multitemporal remotely sensed data provides good conditions and convenience for coastal mapping and change monitoring. Registration of the multisensor and multitemporal remotely sensed imagery is a basic and crucial step for subsequent change monitoring and analysis. Image registration is an important subject in photogrammetry and remote sensing. Many related studies have been reported. In general, it is relatively easy when encountered with good image texture conditions. However, on relatively poor or highly repetitive textural images such as water

Received 29 May 2012; accepted 15 November 2013.

Address correspondence to Liang Cheng, Jiangsu Provincial Key Laboratory of Geographical Information Science and Technology, Nanjing University, Nanjing, 210093, China. E-mail: lcheng@nju.edu.cn

Color versions of one or more of the figures in the article can be found online at www.tandfonline.com/umgd.

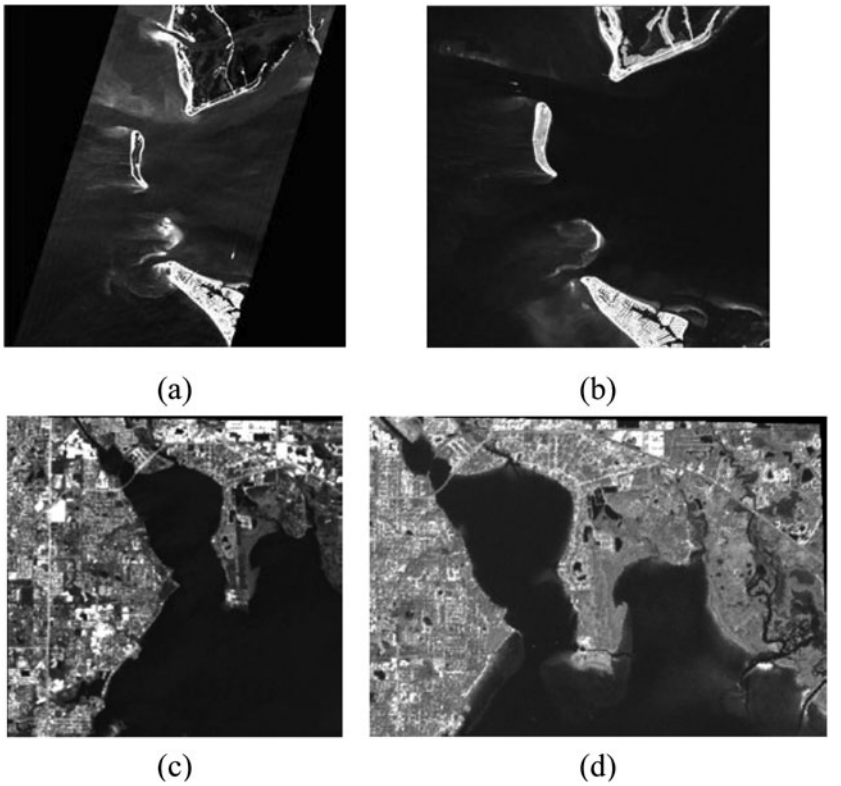

Figure 1. Two typical examples of remotely sensed images with poor textures in coastal area for image registration.

bodies, forestry areas, and dense city centers, image registration is a difficult and challenging problem (Zhu 2007; Wu 2012).

Coastal area is a typical poor-texture scene with a proportion of water area, where images with few or homogeneous textures hardly provides sufficient information for available feature detection and matching. Figure 1 shows two typical examples of coastal remotely sensed images with poor textures, acquired at Tampa Bay, United States. Figure 1(a, b) is a pair of images acquired from different sensors. Figure 1(a) is a part of an EO-1 Hyperion image (band 30), with a resolution of 30m, acquired at 2004/4/2 15:52. Figure 1(b) is a part of a Landsat ETM+ pan image, with a resolution of 15m, acquired at 2003/2/11 15:50. Figure 1(c and d) is another pair of images. Figure 1(c) is a part of a Landsat 5 TM (band 7) covering several islands, with a resolution of 30m, acquired at 2010/4/27 15:52. Figure 1(d) is a part of a Landsat ETM+ pan image covering several islands and a land part, with a resolution of 15m, acquired at 2003/2/11 15:50. Both of two pairs cover a large proportion of water area. Image registration may easily fail in these areas due to homogeneous and low contrast textures, featureless patterns.

Local invariant features, especially affine invariant features, have been shown to be well suited to matching, recognition, and other applications (Mikolajczyk and Schmid 2004). Mikolajczyk et al. (2005) conducted an experiment to compare several affine covariant region detectors, including Harris-Affine, Hessian-Affine, MSER, IBR, EBR, and Salient Regions, and introduced that in many cases the Maximally Stable Extremal

Region (MSER) algorithm can obtain the much better results than the other approaches, by measuring against changes in viewpoint, scale, illumination, defocus, and image compression. Mikolajczyk and Schmid (2005) also compared several local descriptors and identified that Scale-Invariant Feature Transform (SIFT) algorithm can obtain the best matching result. Since the MSER and SIFT are respectively the best detector and descriptor, it is a natural idea to combine them to form a matching technique, named Affine Invariant Feature Matching (AIFM). However, image registration may still encounter big difficulties in coastal area, even using AIFM. Human interactions are usually needed to remove the errors in the results when dealing with the registration of coastal remotely sensed imagery. RANdom SAmple Consensus (RANSAC) is a robust estimation method which is widely used. The combination of AIFM and RANSAC is considered for coastal image registration. The key problem of this combination is how to dig potential of RANSAC for AIFM filtering to obtain matching results as best as possible.

To address this problem, a new systemic approach using high-quality AIFM with a filtering technique under shoreline constraint is proposed in this study for coastal remotely sensed image registration (Figure 2). High-quality AIFM is conducted based on affine invariant features, extracted by an algorithm, named ED-MSER, based on the combination of the MSER and SIFT. To filter the results of AIFM, an automatic filtering technique using RANSAC with shoreline constraint is presented, in which the core issue is how to determinate an appropriate threshold for RANSAC. A progressive threshold strategy (from small value to large value) is presented to determine an appropriate RANSAC threshold. This progressive process is guided by shoreline constraint, helping to determine the appropriate RANSAC threshold in fully automatic way. This RANSAC threshold ensures that the filtering process reaches its objective, which is to remove all wrong matches and simultaneously keep as many correct matches as possible.

Related Work

Registration of Coastal Remotely Sensed Images

A few contour–based approaches have been reported for image registration of remotely sensed images with water area. A contour–based approach to multisensor image registration was proposed by Li et al. (1995). The pairs of closed contour are accepted as candidate matches if the relative differences of their five shape attributes are below a threshold. Salient segments along a contour, such as corners, were used for matching the open contours. Automatic contour- matching technique was introduced by Eugenio and Marqués (2003) for satellite images georeferencing with high accuracy, including estimation of the gradient energy map and detection of the cloudless areas, initialization of the contours positions, and estimation of the transformation parameters using a contour optimization approach. Blokhinov and Gorbachev (2011) presented an approach to matching images based on the technique of comparison of the structure of contours, in which contours are identified based on local salient features of their one-dimensional representation. These methods conduct image matching directly based on contour matching, however, due to fragment, curve and possible low overlap rate, contour matching is in general much more difficult and unreliable than point matching. The more important is, shoreline contour always changes due to its

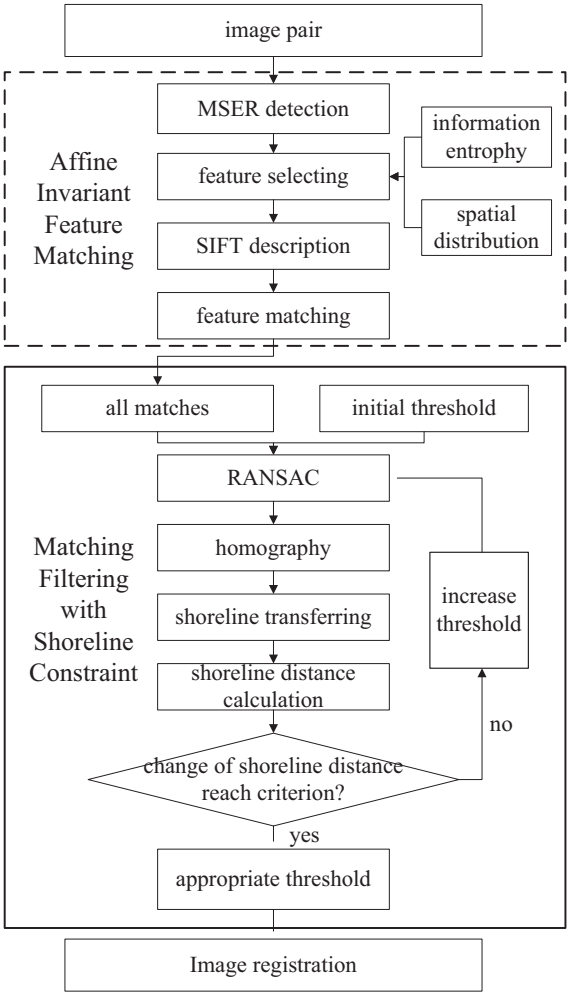

Figure 2. Flow chart of the proposed technical framework.

natural dynamic characteristic, it is not appropriate to be used as the basis of matching in many cases.

Some other efforts have been brought to image registration of coastal remotely sensed images. Ferguson et al. (2006) introduced an approach for automated thematic registration of coastwatch and AVHRR images. This approach converted AVHRR Channel 1 and 2 data to a land and water thematic image, found the offset to maximize classification accuracy, and repositioned the AVHRR and SST images. Song et al. (2010) improved the correctly matching rate in coastal area through retrofitting the descriptor of a SIFT and developing a new similarity measure function based on trajectories generated from Lissajous curves. Liu et al. (2012) introduced a robust point matching RSOC based on two-way spatial order constraints and two decision criteria restrictions and considers both local and global information to reduce ambiguity in matching feature points for images with large area of water. However, these current methods only take account of interest point matching, while

the unique contour features in coastal area are not used. The potential contributions of contour or edge information to the image matching are not fully exploited. In addition, generally, studies related to automatic registration of coastal remotely are quite inadequate.

Affine Invariant Feature Technology in Remotely Sensed Image Matching

A review on affine covariant region detectors was introduced by Mikolajczyk et al. (2005). A comparative study of several local descriptors, including steerable filters, differential invariants, moment invariants, complex filters, and SIFT, was presented by Mikolajczyk and Schmid (2005). Affine invariant feature technology has been successfully applied to remote sensing image matching.

Cheng et al. (2008) presented a method for robust affine invariant feature extraction for image matching, which combines MSER, SIFT, and a selection process based on entropy and spatial distribution. Shah et al. (2008) applied invariant-based similarity by means of template matching to register satellite images for hydrologic change detection in the Arctic. Sirmacek and Unsalan (2009) used SIFT and graph theory applied to IKONOS images for urban-area and building detection. An approach to detect interest points for registration of hyperspectral imagery was introduced by Mukhrjee et al. (2009). To identify geometrically transformed and signal processed images for a given test image, Awrangjeb and Lu (2009) explored the use of different techniques in three main stages (feature detection, feature representation, and feature matching) and proposed a number of promising approaches by combining different techniques of the three stages. Goncalves et al. (2011) proposed a method for automatic image registration based on image segmentation and SIFT, complemented by a robust procedure of outlier removal. Wu et al. (2011) orientated wide-baseline images by incorporating the SIFT algorithm with the RANSAC approach, upon which features are matched based on the self-adaptive triangle constraint. Awrangjeb et al. (2012) presented a framework of contour-based corner detection and discussed two major issues—curve smoothing and curvature estimation—which have major impacts on the corner detection performance. For coastal images, shorelines are the obvious contours, from which corners can be extracted. Based on these extracted corners plus SIFT, it is a way for image matching. But if only using the corners extracted from shorelines, it cannot reach to a good matching results for a whole remotely sensed image, which covers more than shorelines, because the features used for matching should be in a good spatial distribution. Some other related studies have also been reported (Yi et al. 2008; Li et al. 2009; Di et al. 2011; Liu et al. 2012). In general, this technology can achieve good results of image matching when dealing with images with good texture and small changes of view angle. However, for images with poor texture or large changes of view angle, the power of this technology on image matching significantly decreases.

Methodology

High-quality Affine Invariant Feature Matching

From remotely sensed images, shorelines are derived according to the following two steps:

- *Water body extraction*. Mature technologies are used here to extract water body from remotely sensed images. For example, water body can be extracted from Landsat TM images by using NDWI (Mcfeeters 1996) and from Hyperion images by using the method proposed by (Wang and Tian 2008).

- *Shoreline extraction*. Based on the extracted water body information, Edison detector is suggested for shoreline extraction. A small amount of manual editing work may then be needed, in some cases, for deriving a close and clear shoreline, which is used for the subsequent process.

Due to water area can afford little information for image registration, the derived shoreline is used as a land mask to filter the original image, thus removing water area and reserving land area for affine invariant feature extraction. Based on the integration of MSER (the best detector) and SIFT (the best descriptor), an algorithm, named ED-MSER (Cheng et al. 2008), for high-quality affine invariant feature extraction is used. The ED-MSER algorithm can be summarized in the following steps:

- Use standard MSER to detect local affine invariant region. ED-MSER for affine region detection accepts the same input and output as the standard MSER detector.
- Evaluate and select local regions detected by MSER based on entropy and spatial dispersion quality. The features with low information entropy and bad distribution are removed; only the features with high information entropy and good distribution are reserved.
- Use SIFT as ED-MSER descriptor.

The key step in above three steps is the second step. Considering the information content and spatial dispersion quality, the evaluation of features detected by MSER is as follows.

- Take a feature (local region) as a region of interest and create its mask.
- Multiply the original image with the mask to get a new image named as Region of Interest (ROI) image.
- Set the probability of gray value 0 in the ROI image to 0. (4) Calculate entropy of the result image using Formula
- to get entropy of the feature.
- Calculate the threshold of entropy t_1 according to the number of features needed to be removed (remove the features with very low entropy, approximately 20%). Remove the features in which information entropy is less than t_1.
- Partition the whole image: divide the image into nine grid cells (3×3).
- In each grid, calculate spatial dispersion quality $Disp_i$ of features selected using Formula (2). If length of grid cell is l, the threshold of the spatial dispersion quality d is set to $l/4$. If the spatial dispersion quality is larger than d, then the feature selection in this grid cell terminates; else if the spatial dispersion quality is less than d, then replace the feature nearest the central point with another feature with high entropy.

From the above steps, the high-quality affine invariant features are extracted and used in the subsequent image matching processing.

$$H = -\sum_i P_i \, log_2 \, P_i \tag{1}$$

where P_i is the probability of i.

$$Disp = \sqrt{\frac{\sum_{i=1}^{n} (x_i - x_{wmc})^2 + \sum_{i=1}^{n} (y_i - y_{wmc})^2}{n}} \tag{2}$$

$$(\overline{x_{wmc}}, \overline{y_{wmc}}) = \left(\frac{\sum_{i=1}^{n} w_i x_i}{\sum_{i=1}^{n} w_i}, \frac{\sum_{i=1}^{n} w_i y_i}{\sum_{i=1}^{n} w_i} \right)$$

where w_i is weight of point I; entropy of local region is taken as weight.

After feature extraction, the criterion of similarity measure is essential in feature matching. For each feature, in general, the best candidate corresponding match is found by identifying its nearest neighbor in the corresponding image. However, many features may not have any correct match in the corresponding image. A more effective measure is established by comparing the distance of the closest neighbor to that of the second-closest neighbor. If the ratio of shortest distance to second-shortest distance is less than a threshold (0.6 in this study), the two features are considered to be matched. However, there are still many incorrect matches in actual processing. These incorrect matches directly affect the quality and precision of image registration.

AIFM Filtering with Shoreline Constraint

Based on the results of high-quality AIFM in the previous section, the objective of this section is to filter all wrong matches and simultaneously keep as many correct matches as possible. To implement it, a new algorithm to filter the AIFM matches by RANSAC with shoreline contour constraint is proposed, which is performed fully automatically. RANSAC is used to discard wrong matches from correct matches, during which homography is selected as geometric constraint model of RANSAC. In this processing, the key problem is how to determine an appropriate distance threshold, called RANSAC threshold, to dig potential of RANSAC for AIFM filtering to obtain matching results as best as possible. Because a relatively strict RANSAC threshold could remove all wrong matches but also remove too many correct matches, a relatively loose RANSAC threshold may keep many matches but cannot remove all wrong matches.

Therefore, a progressive strategy for RANSAC threshold (from small value to large value) is presented here. The minimum threshold value is firstly taken for RANSAC (none matches or only a few correct matches), and then an initial homograph is calculated. The subsequent progressive process could bring in more correct matches, but its process should be terminated before wrong matches appear. The right stop time is determined by the shoreline constraints. A shoreline can be transferred from a source image to a reference image by homograph. The distance between the transferred shoreline and the corresponding shoreline can be calculated. During the RANSAC iteration using the progressive threshold values, an appropriate RANSAC threshold can be determined in fully automatic way by analyzing the change of this shoreline distance. Based on this threshold, all matches are finally divided into inliers and outliers by RANSAC. This inliers are the final matches using this filtering by RANSAC with shoreline contour constraint.

The dynamic characteristic of shoreline is the reason for the use of shoreline distance change analysis. Because the natural gaps exist in shorelines derived from multi-temporal remotely sensed images, in theory, the minimum shoreline distance cannot be taken as the best constraint for image registration. The analysis of shoreline distance change can work according to the homograph–based rule. That serious error could occur in homography estimation and lead to abrupt changes in shoreline distance values, even if only a few serious mismatches appear in matching results (obvious errors in spatial distribution and seriously inconsistent with other features in geometric constraints). From this, we can know

if the shoreline distance is abruptly changed to a larger value, a few serious mismatches must begin to appear in the results of feature matching. It is the time to finish the RANSAC iteration. This RANSAC threshold ensures that all wrong matches can be removed while also simultaneously keeping as many correct matches as possible.

The detailed procedures of this AIFM filtering are listed as followed.

Step 1: For a pair of images, extract high-quality affine invariant features by using ED-MSER algorithm, respectively, and then conduct affine invariant feature matching.

Step 2: Assign a small value as an initial threshold $TR_{current}$ (1E-2) for RANSAC algorithm and start the first RANSAC iteration. Here the $TR_{current}$ value is assign a small value, as the use of a small threshold can remove all the wrong matches.

Step 3: Determine the inliers and outliers by RANSAC according to the threshold and calculate homograph using the determined inliers.

Step 4: For a shoreline in a source image, create nodes on it according to an interval value. Transfer these nodes from its source image to the reference image by homograph using Formula (3), and form a transferred shoreline by connecting these transferred nodes.

Step 5: Calculate distance value between the transferred shoreline and the reference one. Pick the transferred shoreline as a baseline, draw transect lines perpendicular to its reference shoreline from nodes created in step 4, and calculated average distance value of these transect lines between the two shorelines, named shoreline distance.

Step 6: Calculate RANSAC threshold $TR_{current}$ by Formula (4), and then go to Step 3 and start a new RANSAC iteration. Shoreline distance is also computed. If the ratio of this shoreline distance value to previous one in iteration is more than a threshold (5 times, in this study), finish this iteration and go to Step 7. If the shoreline distance is larger than 30 times pixels, the iteration fails and should be terminated.

Step 7: Take the $TR_{current}$ at the previous iteration as the final RANSAC threshold. The inliers in this RANSAC processing are used for final matching.

$$\begin{bmatrix} X_2 \\ Y_2 \\ 1 \end{bmatrix} = \begin{pmatrix} H_0 & H_1 & H_2 \\ H_3 & H_4 & H_5 \\ 0 & 0 & 1 \end{pmatrix} \begin{bmatrix} X_1 \\ Y_1 \\ 1 \end{bmatrix} \tag{3}$$

where (X_1,Y_1) is the coordinates of a node in a source shoreline, (X_2,Y_2) is the coordinates of its transferred node, H is the homograph matrix computed in RANSAC processing.

$$TR_{current} = \begin{cases} TR_{previous} * 5 & TR_{current} < 10 \,\&\, n \text{ is odd number} \\ TR_{previous} * 2 & TR_{current} < 10 \,\&\, n \text{ is even number} \\ TR_{previous} + 5 & TR_{current} >= 10 \end{cases} \tag{4}$$

where $TR_{current}$ is the threshold value in the current RANSAC iteration, $TR_{previous}$ is the threshold value in the previous RANSAC iteration, and n is iteration times.

Experiment

Two image pairs in Figure 1, covering different types of coastal areas, with different time and different sensors, are used to evaluate applicability of the proposed approach. Since AIFM has been successfully applied in remote sensing, we compare the proposed approach

Table 1
The matching results of Experiment 1 in Figure 4

		Standard AIFM(without filtering) in Figure 4(e)	The proposed approach (with filtering)		
			Threshold 10 in Figure 4(g)	Threshold 40 in Figure 4(h)	Threshold 45 in Figure 4(i)
Total Matches		27	8	11	12
Correct Matches	Number	10	8	11	11
	Rate	37%	100%	100%	91%
Wrong Matches	Number	17	0	0	1
	Rate	63%	0%	0%	9%

(with filtering) with the standard AIFM (without filtering). In addition, we will evaluate the effect of different threshold values for the filtering technique. The precise and efficiency in image registration process are not emphasis of this study. The focus of this study is on correctness of image matching, which meet the objective of this study (remove all wrong matches and simultaneously keep as many correct matches as possible).

Experiment 1 (Figure 1a and b)

Figures 1a and b are used in Experiment 1. Figures 3a and b illustrate the extracted water body from the EO-1 Hyperion imagery (Figure 1a) and its extracted shorelines by Edison. Figures 3c and d illustrate the extracted water body from the Landsat ETM+ imagery (Figure 1b) and its extracted shorelines by Edison. Figures 4a and b illustrate the derived shorelines from Figures 3b and d. Figures 4c and d show 475 and 1027 affine invariant features extracted from Figure 4a and b by ED-MSER, respectively. The results of standard AIFM are shown in Figure 4e, in which 27 matches are obtained. Using the filtering technique proposed by this study, a progressive threshold value for RANSAC iteration is used. Figure 4f demonstrates the change of shoreline distance under the progressive RANSAC threshold values. When change of the shoreline distance reaches the criterion, the appropriate threshold value is determined. In Figure 4g, the filtering results are obtained by using a relatively strict threshold 10. In Figure 4h, the filtering results are derived by an appropriate threshold 40. Figure 4i shows the filtering results with a relatively loose threshold 45. Table 1 lists the matching results corresponding to Figures 4e, g, h, and i. Figure 4j illustrates the reference shoreline (purple) and three transferred shorelines by different thresholds (red dot shoreline: threshold 10, green shoreline: threshold 40, black shoreline: threshold 45). Figures 4k and m show the final registration scene by matching the two images in Figures 4a and b.

Experiment 2 (Figures 1c and d)

Figures 1c and d are used in Experiment 2. Figures 3e and f illustrate the extracted water body from the Landsat TM imagery (Figure 1c) and its extracted shorelines by Edison. Figures 3g and h illustrate the extracted water body from the Landsat ETM+ imagery (Figure 1d) and its extracted shorelines by Edison. Figures 5a and b illustrate the derived shorelines from Figures 3f and h. Figures 5c and d show 630 and 1638 affine invariant

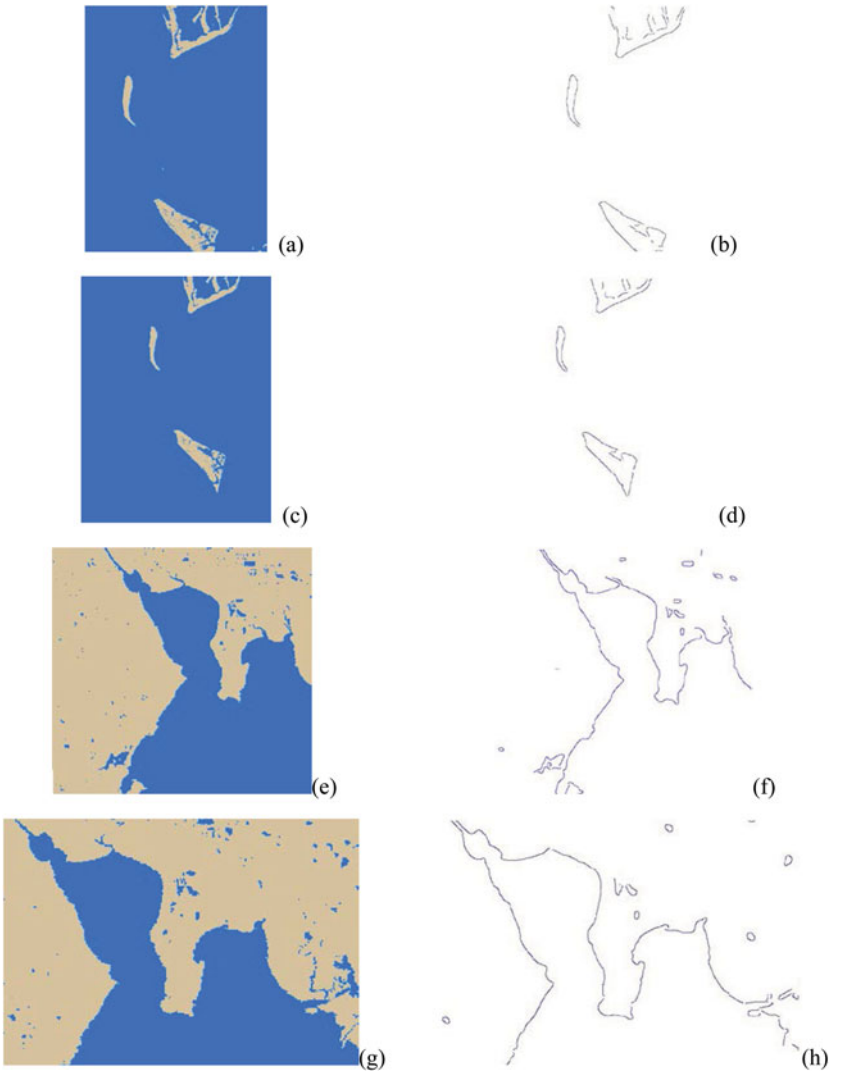

Figure 3. Shoreline extraction. (a) Water body extraction from Figure 1a. (b) Shoreline extraction from (a) by Edison. (c) Water body extraction from Figure 1b. (d) Shoreline extraction from (c) by Edison. (e) Water body extraction from Figure 1c. (f) Shoreline extraction from (e) by Edison. (g) Water body extraction from Figure 1d. (h) Shoreline extraction from (g).

features extracted from Figures 5a and b by ED-MSER, respectively. The results of standard AIFM is shown in Figure 5e, in which 23 matches are obtain. Using the filtering technique proposed by this study, a progressive threshold value for RANSAC iteration is used. Figure 5f demonstrates the change of shoreline distance under the progressive RANSAC threshold values. In Figure 5g, the filtering results are obtained by using a relatively strict threshold 10. In Figure 5h, the filtering results are derived by an appropriate threshold 30. Figure 5i shows the filtering results with a relatively loose threshold 35. Table 2 lists the matching results corresponding to Figures 5e, g, h, and i. Figure 5j illustrates the reference shoreline (purple) and three transferred shorelines by different thresholds (red dot shoreline: threshold

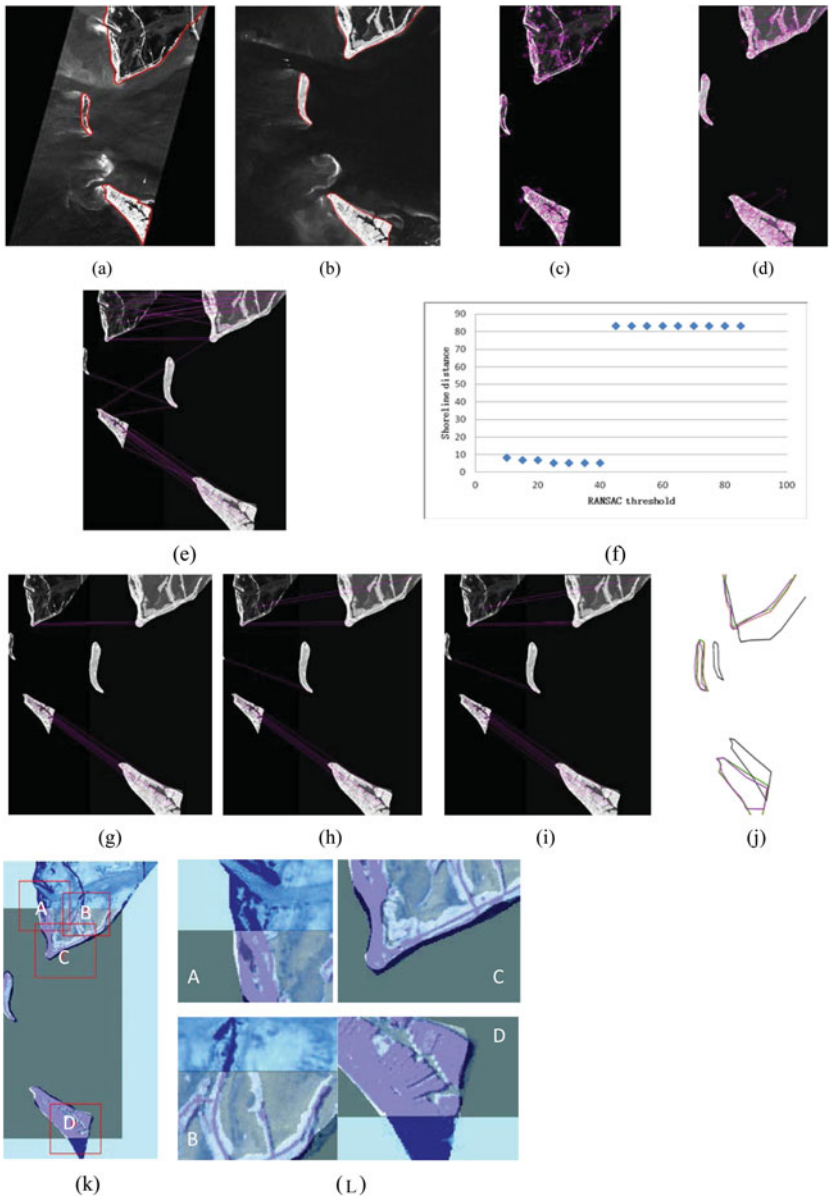

Figure 4. Automatic registration of Figures 1a and b. (a)Hyperion imagery and the derived shorelines, (b) ETM+ imagery and the derived shorelines, (c) 475 affine invariant features extracted from (a), (d) 1027 affine invariant features extracted from (b), (e) The results of AIFM without filtering, (f) Shoreline distance changes with progressive RANSAC threshold values, (g) The filtering results with a relatively strict threshold (10), (h) The filtering results with an appropriate threshold (40), (i) The filtering results with a relatively loose threshold (45), (j) The reference shoreline (purple) and three transferred shorelines (red dot: threshold 10, green: threshold 40, black: threshold 45), (k) The final registration of these two images by filtering with threshold 40, (m) Four details in (k).

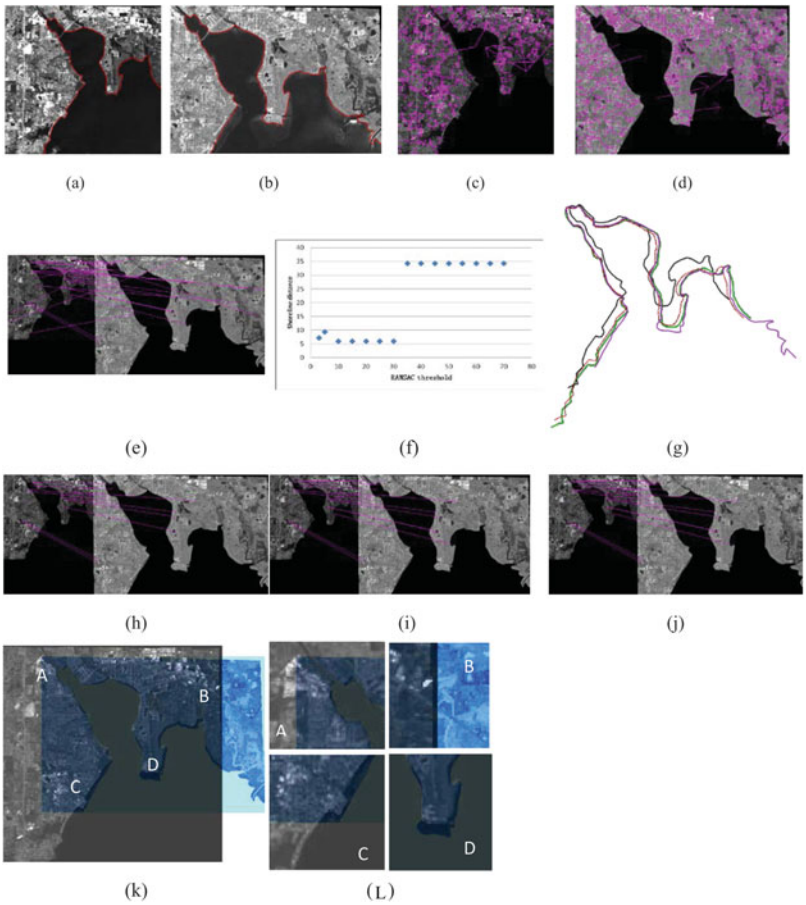

Figure 5. Automatic registration of an image pair (Figures 1c and d). (a) TM imagery and the derived shorelines, (b) ETM+ imagery and the derived shorelines, (c) 630 affine invariant features extracted from (a), (d) 1638 affine invariant features extracted from (b), (e) The results of affine invariant feature matching without filtering, (f) Shoreline distance changes with progressive RANSAC threshold values, (g) The filtering results with a relatively strict threshold 10, (h) The filtering results with the appropriate threshold 30, (i) The filtering results with a relatively loose threshold 35, (j) The reference shoreline (purple) and three transferred shorelines (red dot: threshold 10, green: threshold 30, black: threshold 35), (k) The matched two images by RANSAC filtering with threshold 30, (m) Four details in (k).

10, green shoreline: threshold 30, black shoreline: threshold 35). Figures 5k and m show the final registration scene by matching the two images in Figures 5a and b. From Figure 5k, we can see that two images are matched well in visual check. From the label C and D in Figure 5m, we can find the obvious shoreline changes from the matched two images, which prove it is not appropriate to conduct coastal image registration by using shorelines in many case.

From the two experimental results, we can find the proposed approach (with filtering), even without an appropriate threshold, can reach better matching results than standard AIFM (without filtering). In Experiment 1, all of three types thresholds (relatively strict, appropriate, and relatively loose) lead to a much higher correct matching rate (100%, 100%,

Table 2
The matching results of Experiment 2 in Figure 5

		Standard AIFM(without filtering) in Figure 5(e)	The proposed approach (with filtering)		
			Threshold 10 in Figure 5(g)	Threshold 30 in Figure 5(h)	Threshold 35 in Figure 5(i)
Total Matches		23	10	14	15
Correct Matches	Number	14	10	14	14
	Rate	61%	100%	100%	93%
Wrong Matches	Number	9	0	0	1
	Rate	39%	0%	0%	7%

91%) than standard AIFM (37%). The similar results in Experiment 2, all of three types thresholds (relatively strict, appropriate, and relatively loose) also lead to a much higher correct matching rate (100%, 100%, 93%) than standard AIFM (61%).

Furthermore, during filtering process for AIFM, shoreline constraint guides the detection of an appropriate RANSAC threshold (threshold 40 in Experiment 1, threshold 30 in Experiment 2). In Experiment 1, compared with threshold 40, a smaller threshold 10 can still remove wrong matches but also remove too much correct matches (correct matches decreased from 11 to 8), a larger value (45, the determined appropriate threshold + one step length of progressive process) can increase the number of correct matches but also begin to bring a few wrong matches (wrong matches increased from 0 to 1). Although only one wrong match is brought into the results, the shoreline distance changes from 6 to 83 in Figure 4(f).

In Experiment 2, compared with threshold 30, a smaller threshold 10 can still remove wrong matches but also remove too much correct matches (correct matches decreased from 14 to 10), a larger value (35, the determined appropriate threshold + one step length of progressive process) can increase the number of correct matches but also begin to bring a few wrong matches (wrong matches increased from 0 to 1). Although only one wrong match is brought into the results, the shoreline distance changes from 6 to 34 in Figure 5f. The abrupt change of shoreline distance proves the homograph-based rule mentioned above. The rule is a serious error that could occur in homography estimation and lead to abrupt changes in shoreline distance value, even if only a few serious mismatches appear in matching results. From the two experiments, we can see that the proposed approach can determined an appropriate threshold in automatic way. The more important is that with this automatically determined threshold, the proposed approach can reach much better matching results (100% correct matching rate with relatively most correct matches) than standard AIFM technology.

Conclusions

This study proposed a new approach based on AIFM with a filtering technique for automatic registration of remotely sensed image in coastal areas. Based on the results of high-quality AIFM, to filter all wrong matches and simultaneously keep as many correct matches as possible, an automatic filtering technique using RANSAC based on a progressive threshold strategy guided by shoreline constraint is presented. The experiment analyses using typical coastal remotely sensed images with poor textures conveyed the following conclusions:

1. The proposed filtering technique, even with an arbitrary threshold, can lead to a much higher correct matching rate than standard AIFM.
2. An appropriate RANSAC threshold can be determined in automatic way, with which the proposed approach can reach much better matching results (much higher correct matching rate with relatively most correct matches) than standard AIFM.

Future studies will be conducted on high-reliability matching method for remotely sensed image registration and registration improvement using Progressive Sample Consensus. Experiments by using a larger number of images are of interest.

Acknowledgements

Sincere thanks are given for the comments and contributions of anonymous reviewers and members of the editorial team.

Funding

This work is supported by the National Natural Science Foundation of China (Grant No. 41371017, 41001238), and the National Key Technology R&D Program of China (Grant No. 2012BAH28B02).

References

Awrangjeb, M., and G. Lu, 2009. Techniques for efficient and effective transformed image identification. *Journal of Visual Communication and Image Representation* 20(8):511–520.

Awrangjeb, M., G. Lu, and C. S. Fraser, 2012. Performance comparisons of contour-based corner detectors. *IEEE Transactions on Image Processing* 21(9):4167–4179.

Blokhinov, Y. B., and V. A. Gorbachev. 2011. Contour analysis-based matching of ground objects in aerial images. *International Journal of Computer and Systems Sciences* 50(5):766–777.

Cheng, L., J. Gong, X. Yang, C. Fan, and P. Han. 2008. Robust affine invariant feature extraction for image matching. *IEEE Geoscience and Remote Sensing Letters* 5(2):246–250.

Di, K., Z. Liu, and Z. Yue, 2011. Mars Rover localization based on feature matching between ground and orbital imagery, *Photogrammetric Engineering and Remote Sensing* 77(8):781–791.

Eugenio, F., and F. Marque. 2003. Automatic satellite image georeferencing using a contour – matching approach. *IEEE Transactions on Geoscience and Remote Sensing* 41(12):2869–2880.

Ferguson, R. L., C. Krouse, M. Patterson, and J. Hare, 2006. Automated thematic registration of NOAA, coastwatch, and AVHRR images. *Photogrammetric Engineering and Remote Sensing* 72(6):677.

Gonçalves, H., L. Corte-Real, and J. A. Gonçalves, 2011. Automatic image registration through image segmentation and SIFT. *IEEE Transactions on Geoscience and Remote Sensing*, 99:1–12.

Li, Q., G. Wang, J. Liu, and S. Chen, 2009. Robust scale-invariant feature matching for remote sensing image registration. *IEEE Geoscience and Remote Sensing Letters* 6(2):287–291.

Li, H., B. S. Manjunath, and S. K. Mitra, 1995. A contour–based approach to multisensory image registration. *IEEE Transactions on Image Processing* 4(3):320–334.

Li, R., K. Di, and R. Ma, 2002. 3D shoreline extraction from IKONOS satellite imagery. *Journal of Marine Geodesy* 26(1/2):107–115.

Li, R., S. Deshpande, X. Niu, F. Zhou, K. Di, and B. Wu, 2008. Geometric integration of aerial and high-resolution satellite imagery and application in shoreline mapping. *Journal of Marine Geodesy* 31(3):143–159.

Liu, Z., J. An, and Y. Jing, 2012. A simple and robust feature point matching algorithm based on restricted spatial order constraints for aerial image registration. *IEEE Transactions on Geoscience and Remote Sensing* 99:1–14.

Mcfeeters, S. K. 1996. The use of the normalized Difference Water Index (NDWI) in the delineation of open water features. *International Journal of Remote Sensing* 17(7):1425–1432.

Mikolajczyk, K., and C. Schmid, 2004. Scale and affine invariant interest point detectors. *International Journal of Computer Vision* 60(1):63–86.

Mikolajczyk, K., and C. Schmid. 2005. A performance evaluation of local descriptors. *IEEE Transactions on Pattern Analysis and Machine Intelligence* 27(10):1615–1630.

Mikolajczyk, K., T. Tuytelaars, C. Schmid, A. Zisserman, and J. Matas, 2005. A comparison of affine region detectors. *International Journal of Computer Vision* 65(1/2):43–72.

Mukhrjee, A., M. Velez-Reyes, and B. Roysam. 2009. Interest points for hyperspectral image data. *IEEE Transanctions on Geoscience and Remote Sensing* 47(3):748–760.

Shah, C. A., Y. Sheng and L. C. Smith. 2008. Automated image registration based on pseudo invariant metrics of dynamic land-surface features. *IEEE Transactions on Geoscience and Remote Sensing* 46(11):3908–3916.

Sirmacek, B., and C. Unsalan, 2009. Urban-area and building detection using SIFT keypoints and graph theory. *IEEE Transactions on Geoscience and Remote Sensing* 47(4):1156–1167.

Song, Z., S. Li, and T. F. George, 2010. Remote sensing image registration approach based on a retrofitted SIFT algorithm and Lissajous-curve trajectories. *Optics Express* 18(2):513–522.

Wang, X. C., and Q. J. Tian, 2008. Autoclassifying water bodies in LiaoDong Bay based on model of double absorption depth. *Remote Sensing Technology and Application* 23(1):42–46.

Wu, B., Y. Zhang, and Q. Zhu, 2011. A triangulation-based hierarchical image matching method for wide-baseline images. *Photogrammetric Engineering and Remote Sensing*, 77(7):695–708.

Wu, B., Y. Zhang, and Q. Zhu, 2012. Integrated point and edge matching on poor textural images constrained by self-adaptive triangulations. *ISPRS Journal of Photogrammetry and Remote Sensing*, 68:40–55.

Yi, Z., C. Zhiguo, and X. Yang, 2008. Multi-spectral remote image registration based on SIFT. *Electronics Letters* 44(2):107–108.

Zitova, B., and J. Flusser, 2003. Image registration methods: A survey. *Image and Vision Computing* 21(11):977–1000.

Zhu, Q., B. Wu, and Y. Tian, 2007. Propagation strategies for stereo image matching based on the dynamic triangle constraint. *ISPRS Journal of Photogrammetry and Remote Sensing*, 62(4):295–308.